

# Triplet Sensitized Photolysis of a Vinyl Azide: Direct Detection of a Triplet Vinyl Azide and Nitrene

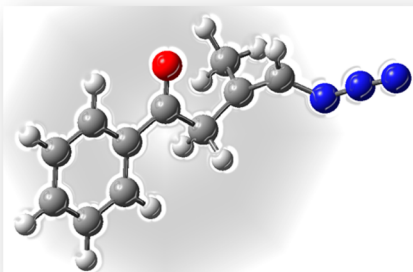
Sridhar Rajam,<sup>†</sup> Abhijit V. Jadhav,<sup>†</sup> Qian Li,<sup>†</sup> Sujan K. Sarkar,<sup>†</sup> Pradeep N. D. Singh,<sup>†</sup> Ahleah Rohr,<sup>†</sup> Tamara C. S. Pace,<sup>‡</sup> Rui Li,<sup>‡</sup> Jeanette A. Krause,<sup>‡</sup> Cornelia Bohne,<sup>‡</sup> Bruce S. Ault,<sup>†</sup> and Anna D. Gudmundsdottir<sup>\*,†</sup>

<sup>†</sup>Department of Chemistry, University of Cincinnati, Cincinnati, Ohio 45221-0172, United States

<sup>‡</sup>Department of Chemistry, University of Victoria, P.O. Box 3065, Victoria, BC V8W 3 V6, Canada

## S Supporting Information

**ABSTRACT:** Photolysis of vinylazide **1**, which has a built-in acetophenone triplet sensitizer, in argon-saturated toluene results in azirine **2**, whereas irradiation in oxygen-saturated toluene yields cyanide derivatives **3** and **4**. Laser flash photolysis of azide **1** in argon-saturated acetonitrile shows formation of vinylnitrene **1c**, which has a  $\lambda_{\text{max}}$  at  $\sim 300$  nm and a lifetime of  $\sim 1$  ms. Vinylnitrene **1c** is formed with a rate constant of  $4.25 \times 10^5 \text{ s}^{-1}$  from triplet 1,2-biradical **1b**. Laser flash photolysis of **1** in oxygen-saturated acetonitrile results in **1c-O** ( $\lambda_{\text{max}} = 430$  nm,  $\tau \approx 420 \mu\text{s}$  acetonitrile). Density functional theory (DFT) calculations were used to aid in the characterization of the intermediates formed upon irradiation of azide **1** and to validate the proposed mechanism for its photoreactivity.

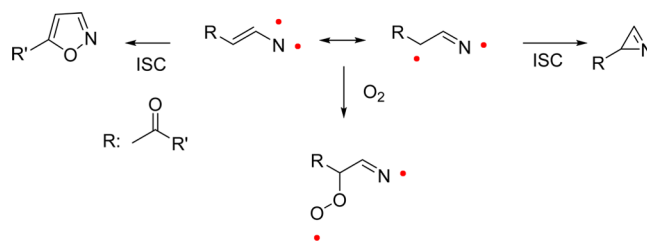


## 1. INTRODUCTION

Nitrenes are fascinating reactive intermediates that have been used in various applications such as photoaffinity labeling, cross-linking of polymers, and surface modifications, and they also have potential as building blocks for high-spin assemblies and are therefore of general interest.<sup>1,2</sup> Because nitrenes are used in such a broad variety of applications, it is important to determine how they can be formed selectively and to identify the factors that control their reactivity. Generally, the reactivity of nitrenes is controlled by their spin configuration, as nitrenes with singlet configuration are generally short-lived and highly reactive, whereas their triplet counterparts are more stable and less reactive. However, it is not only the electronic configuration that controls the reactivity of nitrenes but also their substitution. Recently, we reported the first direct detection of triplet vinylnitrenes in solution by performing laser flash photolysis studies of 2H-azirine and oxazole derivatives.<sup>3–5</sup> Triplet vinylnitrenes display unique reactivity among nitrenes, as they are short-lived intermediates with lifetimes of a few microseconds. Vinylnitrenes decay by intersystem crossing to yield azirines, although vinylnitrenes that have a  $\gamma$ -carbonyl group intersystem cross to form isoxazole derivatives in competition with formation of azirines.<sup>3,4,6</sup> The singlet–triplet energy gap in vinylnitrenes has been calculated to be  $\sim 15$  kcal/mol.<sup>7</sup> On the basis of this, the lifetimes of triplet vinylnitrenes are limited by their rate constant for intersystem crossing to their singlet products, which for the triplet vinylnitrene is on the order of  $10^5$ – $10^6 \text{ s}^{-1}$ . Another unique property of triplet vinylnitrenes is that they react efficiently with oxygen, due to their significant 1,3-

biradical character (Scheme 1), to form an intermediate with a new C–O bond.<sup>4</sup>

### Scheme 1



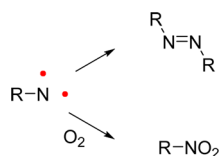
In comparison, triplet nitrenes with electron-donating substituents, such as alkyl- and phenylnitrenes, are long-lived intermediates with lifetimes of several milliseconds in solution.<sup>8,9</sup> Triplet alkyl- and aryl nitrenes are highly unreactive because they do not undergo intersystem crossing to react with themselves nor the solvent but rather they decay by dimerizing to form azo compounds (Scheme 2).<sup>8–11</sup> Additionally, because they do not have carbon atoms with unpaired electrons, triplet alkyl- and aryl nitrenes react with  $\text{O}_2$  to form the corresponding nitro-compounds.

The most common precursor for nitrenes is the corresponding azido compound that can be activated either thermally or

Received: August 17, 2014

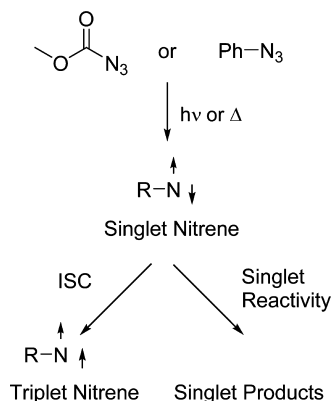
Published: August 27, 2014

Scheme 2



photochemically. For example, singlet aryl- and alkoxy nitrenes are formed by direct photolysis of the corresponding azido precursors that intersystem cross to form the ground-state triplet nitrenes.<sup>2</sup> The singlet–triplet energy gap in alkoxy nitrene has been reported in the 3–8 kcal/mol range, and alkoxy nitrene intersystem crosses with a rate constant of  $\sim 10^8$  s<sup>-1</sup> from its singlet to its triplet.<sup>12</sup> In comparison, in phenylnitrene the singlet–triplet energy gap is 14.8 kcal/mol,<sup>13</sup> and it intersystem crosses with a rate constant of  $\sim 3 \times 10^6$  s<sup>-1</sup> at cryogenic temperatures (Scheme 3).<sup>14</sup> Alkyl nitrenes, however, cannot be

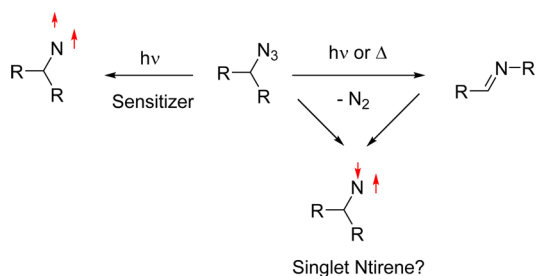
Scheme 3



formed by direct photolysis of azidoalkanes because direct photolysis yields imine products by either concerted reactions in the singlet excited state or through short-lived singlet nitrenes that form the imine products faster than they can intersystem cross to the more stable triplet.<sup>8,15</sup> The energy gap between singlet and triplet alkyl nitrenes has been reported to be on the order of 31.2 kcal/mol,<sup>16</sup> and thus intersystem crossing is expected to be slow. Hence, triplet alkyl nitrenes can only be formed by intra- or intermolecular sensitization of azidoalkanes (Scheme 4).<sup>8</sup>

In this article, we demonstrate that a vinylazide with a built-in triplet sensitizer can serve as a precursor to triplet vinyl nitrenes. Photolysis of azide **1** in argon-saturated solutions yields azirine **2**, whereas in oxygen-saturated solutions **3** and **4** are formed. Laser flash photolysis of azide **1** in argon-saturated

Scheme 4

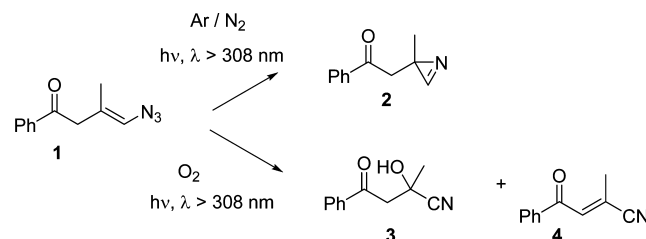


solutions yields 1,2-biradical **1b**, which extrudes a N<sub>2</sub> molecule to form triplet vinyl nitrene **1c**. The latter then slowly intersystem crosses to form azirine **2**. In oxygen-saturated acetonitrile solutions, laser flash photolysis shows that **1b** is intercepted to form peroxide radical **1c-O**. In cryogenic argon matrices irradiation of vinyl azide **1** yields benzoic and imine radicals.

## 2. RESULTS

**2.1. Product Studies.** Irradiation of vinyl azide **1** in argon-saturated toluene via Pyrex filter resulted in **2** as the only product (Scheme 5). The photolysis of vinyl azide **1** was followed by <sup>1</sup>H

Scheme 5



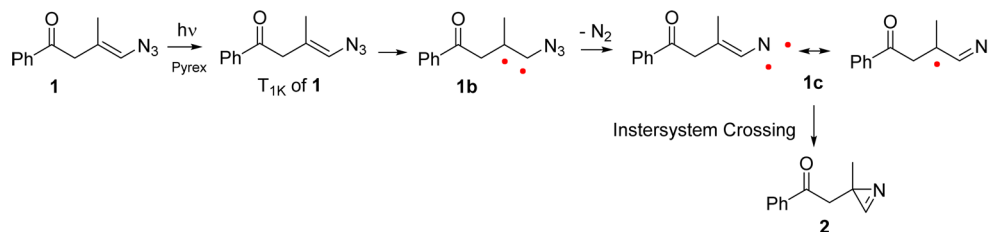
NMR spectroscopy, which showed that vinyl azide **1** is converted selectively to **2**. Photolysis of vinyl azide **1** in oxygen-saturated toluene did not yield azirine **2** but resulted in **3** and **4** (Scheme 5).

From the product studies we theorize that irradiation of vinyl azide **1** forms the first triplet excited state of the ketone ( $T_{1K}$ ) of **1**, which then undergoes energy transfer to yield biradical **1b**. Extrusion of a N<sub>2</sub> molecule from **1b** results in vinyl nitrene **1c**, which intersystem crosses to form **2** (Scheme 6). In comparison, we propose that in oxygen-saturated solutions **1b** is formed and trapped with oxygen to form **1b-O** that expels a N<sub>2</sub> molecule to form **1c-O**, which results in formation of **3** and **4** (Scheme 7). It was not possible to isolate the peroxide precursor to **3** (Scheme 7) using silica column chromatography.

**2.2. Molecular Modeling.** To support the reaction mechanisms for vinyl azide **1** proposed in Schemes 6 and 7, we performed calculations using Gaussian03 at the B3LYP level of theory with the 6-31+G(d) basis set.<sup>17–19</sup> The optimized structure of vinyl azide **1** is very similar to its X-ray crystal structure (Figure 1). Time-dependent density functional theory (TD-DFT) calculations of vinyl azide **1** place the first triplet excited ( $T_{1K}$ ) and second triplet excited ( $T_{2K}$ ) states of the ketone of **1** at 74 and 76 kcal/mol, respectively, above the  $S_0$  of **1**. The energies of  $T_{1K}$  and  $T_{2K}$  are similar to those reported for valerophenone derivatives.<sup>20</sup> Visualization of the molecular orbitals revealed, as expected, that  $T_{1K}$  of **1** has a ( $n, \pi^*$ ) configuration of the acetophenone moiety, and it is  $\sim 3$  kcal/mol more stable than the second excited state ( $T_{2K}$ ) of the ketone with a ( $\pi, \pi^*$ ) configuration.

As the  $T_{1K}$  of **1** is the lowest triplet excited state of the ketone chromophore, it is possible to optimize its structure. The optimized structure of  $T_{1K}$  of **1** is located 65 kcal/mol above the ground state ( $S_0$ ) of **1**; this is considerably lower than the energy obtained from TD-DFT calculations. However, DFT calculations are known to underestimate the triplet energy of ketones with a ( $n, \pi^*$ ) configuration.<sup>21</sup> The C–O bond in  $T_{1K}$  of **1** is prolonged to 1.29 Å, in comparison to the C=O bond in the  $S_0$  of **1**, which is 1.22 Å. The elongation of the C–O bond fits well with what has been observed for triplet aryl ketones with a ( $n, \pi^*$ ) configuration.<sup>22</sup> The N–N–N angle is almost linear (173°), and the calculated IR stretch for the azido group is 2247 cm<sup>-1</sup>, similar

Scheme 6



Scheme 7

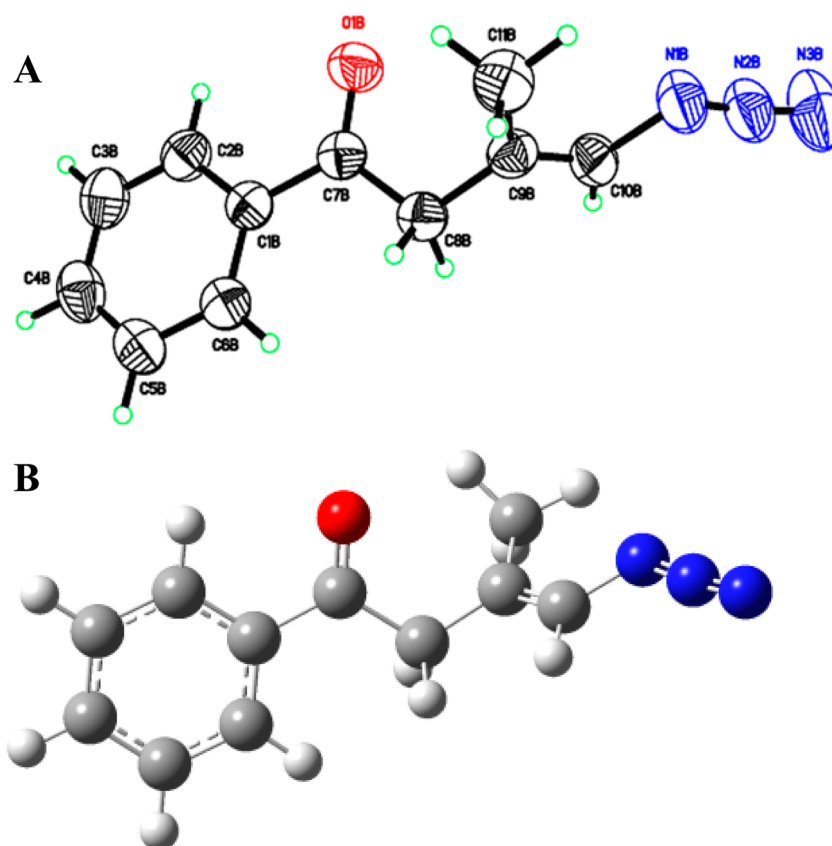
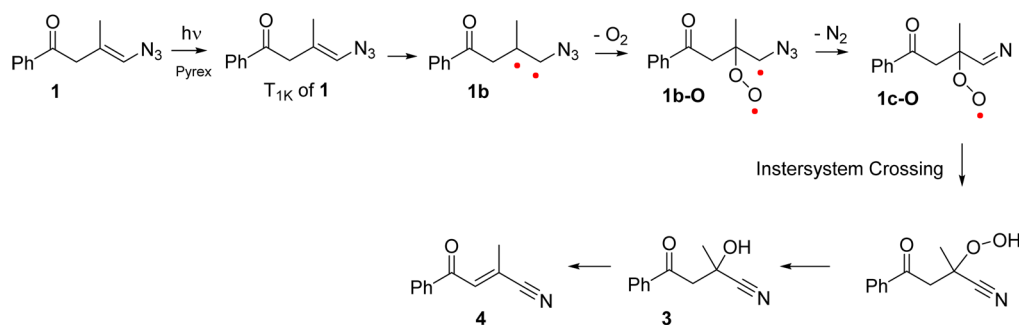


**Figure 1.** (A) Molecular structure of vinyl azide **1** as determined by X-ray analysis. Only one of the two independent molecules is shown here (50% probability ellipsoids). Selected bond distances (Å) and angles (deg): C1A–O7A = 1.217(1), C1B–O7B = 1.221(1), N1A–C10A = 1.423(2), N1B–C10B = 1.422(2), C9A–C10A = 1.322(2), C9B–C10B = 1.322(2), N1A–N2A–N3A = 171.6(2), N1B–N2B–N3B = 171.7(2), O1A–C7A–C8A–C9A = 6.8(2), O1B–C7B–C8B–C9B = 9.8(2), C7A–C8A–C9A–C11A = 73.6(2), C7B–C8B–C9B–C11B = 73.8(1), C8A–C9A–C10A–N1A = –178.6(1), C11A–C9A–C10A–N1A = 1.6(2), C8B–C9B–C10B–N1B = –178.9(1), C11B–C9B–C10B–N1B = 0.7(2), C9A–C10A–N1A–N2A = –168.9(2), C9B–C10B–N1B–N2B = –177.9(1). (B) Optimized structure of **1**.

to what was calculated for the  $S_0$  of **1**; thus, it is postulated that the excited state is localized on the carbonyl group because the azido moiety in  $T_{1K}$  of **1** is similar to the  $S_0$  of **1**. Spin density

calculations demonstrate that the spin density is localized on the carbonyl oxygen atom and the phenyl ring, further supporting the  $(n, \pi^*)$  configuration for  $T_{1K}$  of **1** (Figure 2).

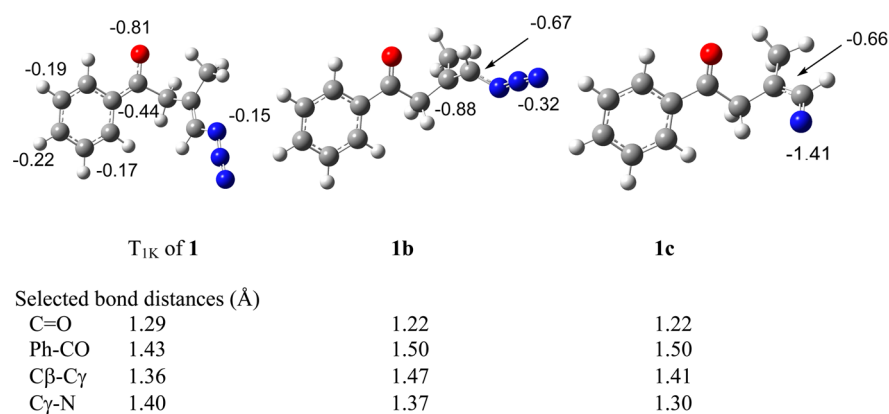


**Figure 2.** Optimized structure of  $T_{1K}$  of **1**, triplet biradical **1b**, and triplet vinylnitrene **1c**. The calculated bond distances are in Å. The calculated spin densities are written next to the corresponding atoms.

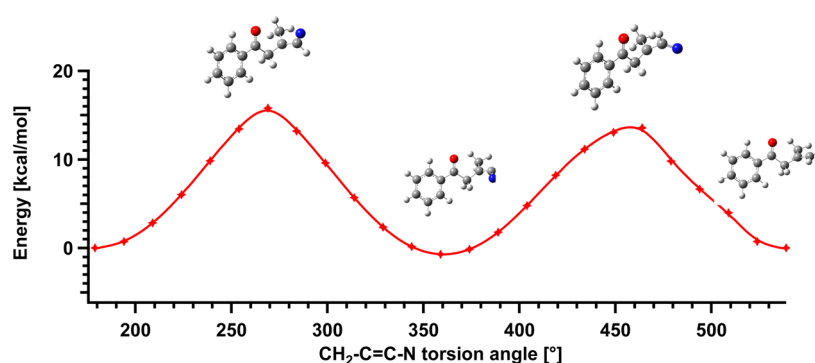


**Figure 3.** Calculated rotational barrier around the  $\text{CH}_2\text{-C}=\text{C}\text{-N}$  bond in triplet vinylnitrene **1c**.

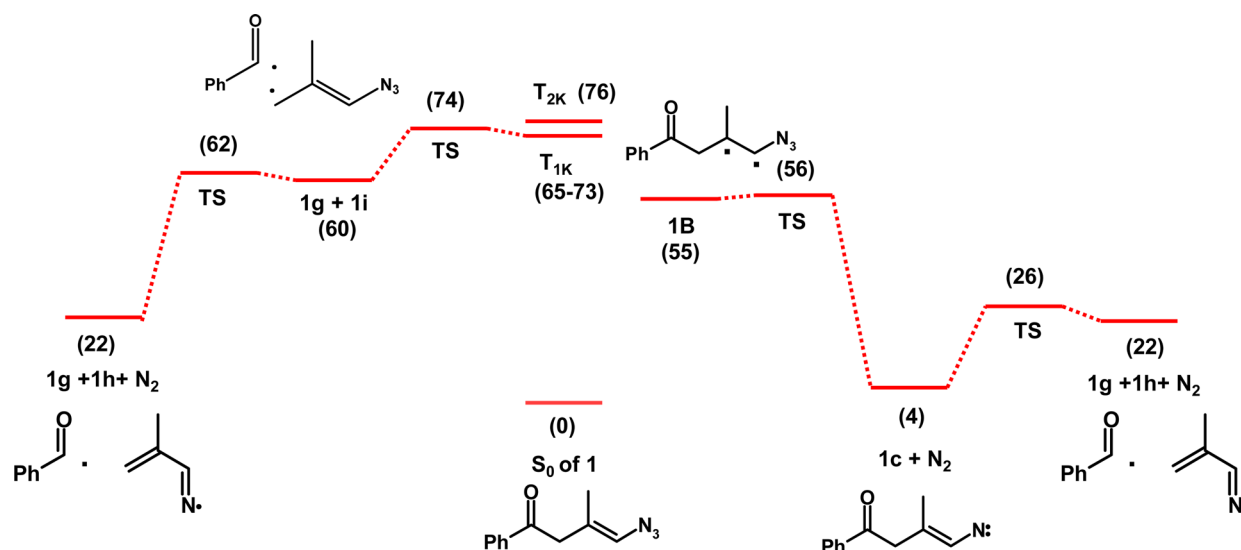


**Figure 4.** Calculated stationary points on the triplet surface of **1**. Numbers in parentheses are energies in kcal/mol. The energies of  $T_{2K}$  of **1** and  $T_{1K}$  of **1** (65) were obtained by TD-DFT calculations, and the other ones were obtained by optimization calculations.

The optimized structure of triplet 1,2-biradical **1b** is located at 55 kcal/mol above the  $S_0$  of **1**. The  $C\beta\text{-}C\gamma$  bond length is 1.47 Å, and thus it can be described as having single-bond character, as opposed to the same bond in the  $S_0$  of **1** where it has double-bond character (1.34 Å). The dihedral angle between the  $\text{CH}_3\text{-}C\beta\text{-}C\gamma\text{-H}$  is  $97^\circ$  in **1b**, in order to minimize the overlap between the two adjacent radical centers. Furthermore, the  $\text{C-N}$  bond was shortened to 1.37 Å in **1b**, from 1.42 Å in the  $S_0$  of **1**. The stretching frequency of the azido group is  $2201\text{ cm}^{-1}$  in **1b**,

which is only slightly lower in frequency than that calculated for the azido stretch in the  $S_0$  of **1** of  $2251\text{ cm}^{-1}$ . Spin density calculations further support that **1b** is a 1,2-biradical as the spin densities of the  $C\beta$  and  $C\gamma$  are  $-0.88$  and  $-0.67$ , respectively. The unpaired electron on the  $C\gamma$  is conjugated with the azido moiety as the terminal N atom has a spin density of  $-0.32$ .

Vinylnitrene **1c** and  $\text{N}_2$  molecule are located 4 kcal/mol above the  $S_0$  of **1**. In **1c** the  $\text{C}=\text{C}$  and  $\text{C}=\text{N}$  bond distances are 1.41 and 1.30 Å, respectively, similar to what we have reported

previously for vinylnitrenes using DFT calculations.<sup>3</sup> The calculated spin density of vinylnitrene **1c** demonstrates that the unpaired electrons are located mainly on the N atom ( $-1.41$ ) and the C $\beta$  atom ( $-0.66$ ) (Figure 2). The calculated rotational barrier around the CH<sub>2</sub>-C=C-N bond in vinylnitrene **1c** is displayed in Figure 3. The calculated rotational barriers around the C=C bond of 16 and 14 kcal/mol are very significant.

The calculated stationary points on the triplet surface of **1** are shown in Figure 4. The transition state for forming triplet vinylnitrene **1c** from extrusion of a N<sub>2</sub> molecule from biradical **1b** is located  $\sim 1$  kcal/mol above **1b**. We also calculated the transition states for T<sub>1K</sub> of **1** and vinylnitrene **1c** (Figure 4) to undergo  $\alpha$ -cleavage. The transition state for  $\alpha$ -cleavage of vinylnitrene **1c** is located 22 kcal/mol above **1c** and results in **1g** and **1h**. In comparison, the transition state for T<sub>1K</sub> of **1** undergoing  $\alpha$ -cleavage is located 9 kcal/mol above T<sub>1K</sub> of **1** at 65 kcal/mol and yields **1g** and **1i**. The transition state for **1i** to form **1h** with extrusion of a N<sub>2</sub> molecule is 2 kcal/mol above **1i**. These calculations show that the energies necessary to form biradical **1b** from T<sub>1K</sub> of **1** and vinylnitrene **1c** from biradical **1b** are feasible at ambient temperature. Similarly,  $\alpha$ -cleavage for T<sub>1K</sub> of **1** is expected to be feasible at ambient temperature, although  $\alpha$ -cleavage products were not observed in solution. On the other hand, the transition state barrier for  $\alpha$ -cleavage of vinylnitrene **1c** is significantly larger, and thus this reaction is not expected to take place thermally.

We optimized **1c-S**, the open-shell singlet of **1c**, and established that the singlet-triplet energy gap is 15 kcal/mol. The singlet-triplet energy gap for **1c** is similar to what Parasuk and Cramer calculated for simple vinylnitrene CH<sub>2</sub>=CH-N:<sup>7</sup>

We optimized the structures obtained from **1b** and **1c** reacting with O<sub>2</sub> (Figure 5). Spin density calculations show that peroxide

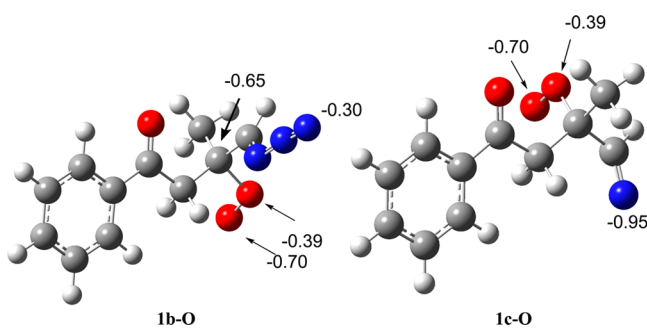


**Figure 5.** Calculated structures of (a) **1b-O** and (b) **1c-O**. The numbers stated are the calculated spin densities.

**1b-O** has a spin density of  $-0.70$  and  $-0.39$  on the peroxide oxygen atoms and  $-0.65$  on the carbon atom adjacent to the azido moiety, which is resonance-stabilized with the terminal N atom in the azido group that has a spin density of  $-0.30$ . In comparison, the spin density of **1c-O** is localized on the N atom and the peroxide oxygen atoms (Figure 5). Finally, we calculated stationary points on the energy surface of **1b** reacting with oxygen. Biradical **1b** can react with oxygen to form biradical **1b-O**, which is 32 kcal/mol more stable than **1b** and O<sub>2</sub> (Figure 6). Biradical **1b-O** can extrude a N<sub>2</sub> molecule to form **1c-O**, which is 40 kcal/mol more stable than **1b-O**. It can also be theorized that the expulsion of N<sub>2</sub> and addition of O<sub>2</sub> to **1b** is concurrent, but due to spin restrictions, we cannot obtain the transition states for **1b** adding to O<sub>2</sub> to form **1b-O** or **1c-O**. The transition state for **1b-O** to expel an N<sub>2</sub> molecule to form **1c-O** is 2 kcal above **1b-O**, and thus similar for **1b** expelling N<sub>2</sub> molecule.

**2.3. Matrix Isolation.** We deposited **1** into argon matrices at 14 K. Two azido bands were observed for **1**, an intense band at 2114 cm<sup>-1</sup> and a band with lower intensity at 2136 cm<sup>-1</sup> (Figure 7a). Presumably, these two bands are due to different conformers of **1** or entrapment of **1** in different matrix sites. After 2 h of irradiation via Pyrex filter, the azido band at 2114 cm<sup>-1</sup> was depleted, whereas the azido band at 2136 cm<sup>-1</sup> was not affected (Figure 7). In addition, bands at 1704, 1691, 1347, 1336, 1298, and 700 cm<sup>-1</sup> were also depleted. The IR spectrum obtained after irradiation showed formation of several new bands, the most significant being at 1826, 1717, 1691, 929, 829, and 746 cm<sup>-1</sup>. We assign the bands at 1826 and 746 cm<sup>-1</sup> (Figure 7b) to benzoyl radical **1g**. The carbonyl group in benzoyl radical has been reported to be at 1828 cm<sup>-1</sup>.<sup>23</sup> The bands at 1717, 1691, 1677, 929, and 829 cm<sup>-1</sup> were attributed to **1h** (Figure 8). The coupled C=N and C=C stretching of **1hA** are calculated to be at 1695 and 1684 cm<sup>-1</sup> and at 1724 and 1670 cm<sup>-1</sup> for **1hB**, whereas the bending of the CH<sub>2</sub> in **1hA** and **1hB** are calculated to be at 948 and 952 cm<sup>-1</sup>, respectively (Figure 7b).

Thus, photolysis of **1** in argon matrices leads to  $\alpha$ -cleavage to form **1g** and **1h**. Because we did not observe any product attributable to benzoyl radical formation in solution, we theorize that vibrationally hot **1c** cleaves to form **1g** and **1h**, rather than **1** undergoing  $\alpha$ -cleavage. This is further supported by our calculations, which demonstrate that in matrices vibrationally hot **1c** is formed with sufficient energy to overcome the transition state barrier to form **1g** and **1h**. There are many examples of azido and nitrene derivatives that have been proposed to react from vibrationally hot states.<sup>24,25</sup> However, we cannot rule out that T<sub>1K</sub> of **1** undergoes  $\alpha$ -cleavage directly. As irradiation of vinyl azide **1** in matrices did not result in any new IR bands that were

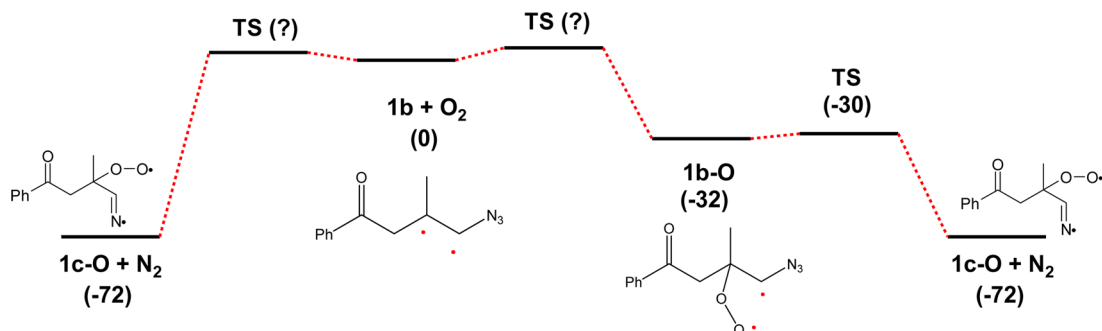


**Figure 6.** Stationary points on the energy diagram for **1b** reacting with oxygen. The numbers in parentheses are energies in kcal/mol.



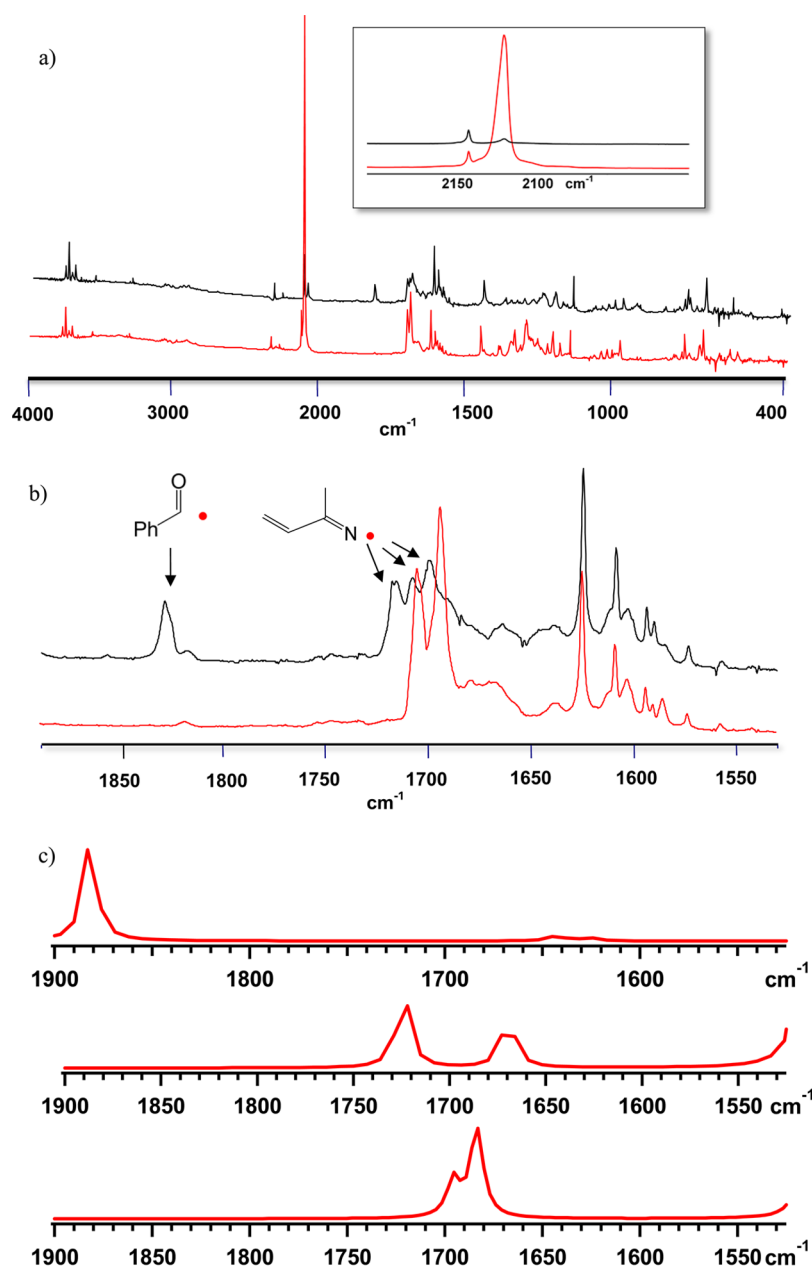


**Figure 7.** (a) Comparison of IR spectra of **1** before (red) and after (black) irradiation in argon matrices. (b) Expansion and (c) calculated spectra of benzoyl and **1hA** and **1hB** radicals.

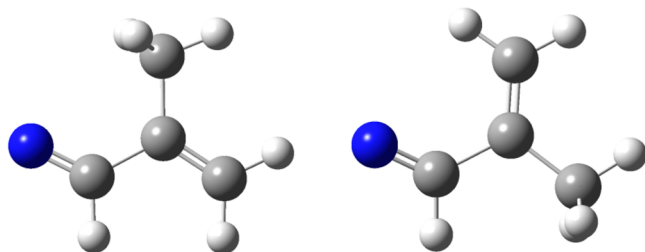


**Figure 8.** Conformers A and B of **1h**.

depleted upon further irradiation, we can rule out vinylnitrene **1c** forming **1g** and **1h** as secondary photoproducts.

**2.4. Laser Flash Photolysis.** Laser flash photolysis studies of **1** in argon-saturated acetonitrile showed a broad transient absorption between 300 and 360 nm (Figure 9a). The transient monitored

at 310 and 330 nm in argon-saturated solvents was formed with a rate constant of  $4.25 \times 10^5 \text{ s}^{-1}$  ( $\tau = 2.4 \mu\text{s}$ ) in acetonitrile and  $3.0 \times 10^5 \text{ s}^{-1}$  ( $\tau = 3.3 \mu\text{s}$ ) in methanol (Figure 10) and had a lifetime on the order of a millisecond ( $\tau \approx 1 \text{ ms}$ ). We assign this transient absorption to have contributions from both **1b** and **1c** based on TD-DFT calculations that place the major electronic transitions for **1b** at 354 ( $f = 0.011$ ), 350 ( $f = 0.034$ ), and 300 ( $f = 0.012$ ) nm and for the two minimal energy conformers of **1c**, **1cA** 332 ( $f = 0.009$ ) and 318 ( $f = 0.005$ ) nm and **1cB** at 323 ( $f = 0.010$ ) and 318 ( $f = 0.018$ ) nm (Figure 11). Furthermore, since the absorption of **1b** and **1c** overlap, **1c** must have stronger absorption than **1b**, as the transient absorption is observed growing in at shorter time scales, suggesting that **1b** forms **1c**. The decay rate constant for **1b** is the same as the rate constant for forming **1c**. Thus, **1b** has a lifetime of  $2.4 \mu\text{s}$  in acetonitrile and it

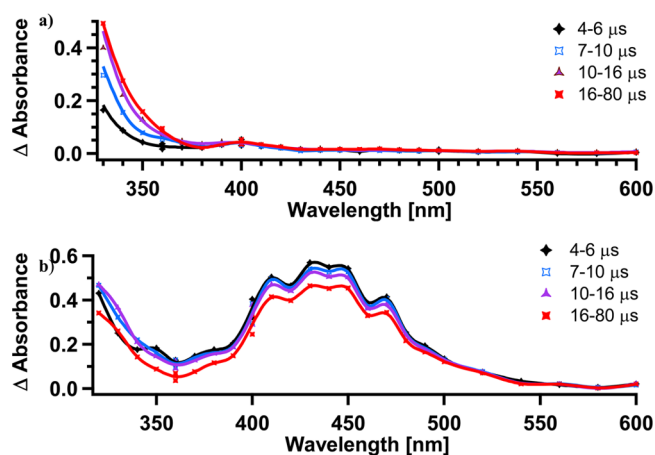


**Figure 9.** Laser flash photolysis of **1** in (a) argon-saturated acetonitrile and (b) oxygen-saturated acetonitrile with 308 nm laser.

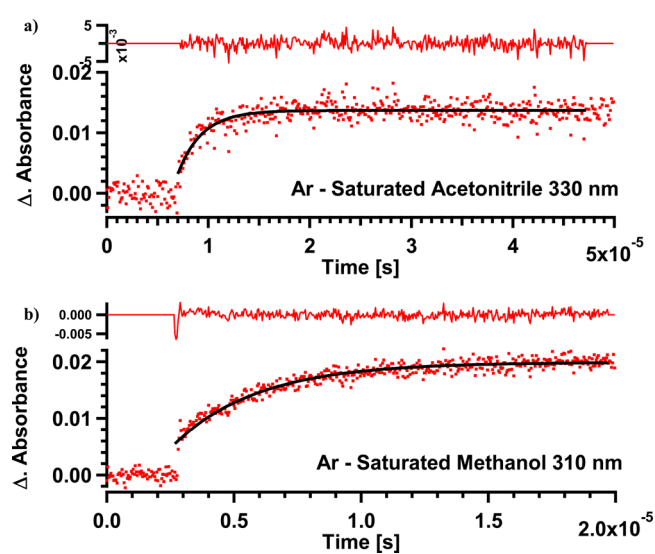


**Figure 10.** Kinetic trace recorded from laser flash photolysis of **1** in argon-saturated (a) acetonitrile at 330 nm and (b) methanol at 310 nm.

decays to form **1c**, which in turn has a lifetime on the order of 1 ms.

To further support the assignment of the transient absorption to vinylnitrene **1c**, we performed laser flash photolysis studies of **1** in oxygen-saturated acetonitrile that resulted in a different transient spectrum with  $\lambda_{\text{max}}$  at 420 nm (Figure 9b). Similar transient absorption was obtained in air-saturated acetonitrile as in oxygen-saturated solutions. We assign this transient to **1c-O** based on its calculated spectrum that has major electronic transitions at 424 nm ( $f = 0.0055$ , Figure 12). Analysis of the kinetics reveals that the absorption forms with a rate constant of  $7.5 \times 10^5 \text{ s}^{-1}$  ( $\tau = 1.33 \mu\text{s}$ ) and  $3.7 \times 10^6 \text{ s}^{-1}$  ( $\tau = 270 \text{ ns}$ ) in air- and oxygen-saturated acetonitrile, respectively. In oxygen-saturated acetonitrile, the transient absorption at 430 nm decayed with a rate constant of  $2.4 \times 10^4 \text{ s}^{-1}$  ( $\tau = 420 \mu\text{s}$ ). As the rate of forming **1c-O** increased at higher  $\text{O}_2$  concentration, we conclude that **1b** reacts with  $\text{O}_2$  to form **1b-O** with a slower rate at the oxygen concentrations employed than **1b-O** expels  $\text{N}_2$ , and thus we only observe the absorption of **1c-O** and not **1b-O**. It can also be theorized that addition of  $\text{O}_2$  to **1b** takes place at the same time as  $\text{N}_2$  extrusion. In addition, the rate constant for forming **1c-O** is  $4.9 \times 10^6 \text{ s}^{-1}$  ( $\tau = 204 \text{ ns}$ ) in oxygen-saturated

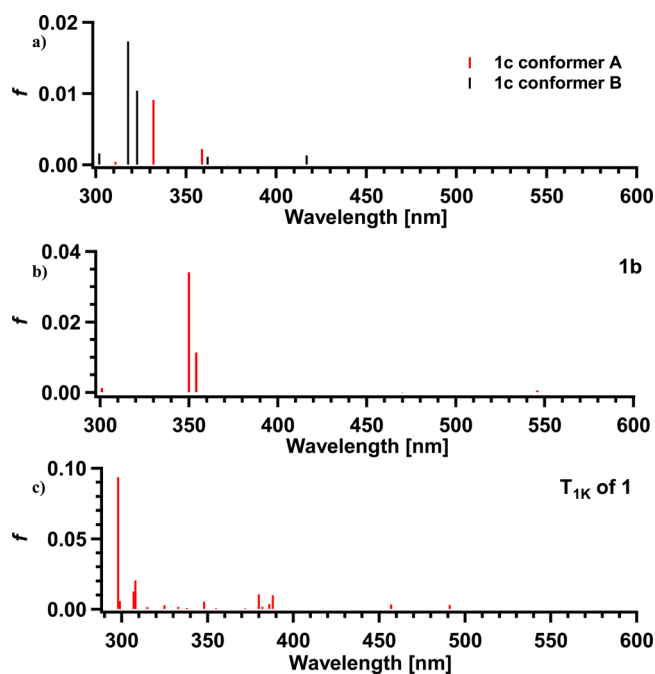


**Figure 11.** Calculated TD-DFT spectra of (a) **1c**, (b) **1b**, and (c)  $T_{1K}$  of **1**.

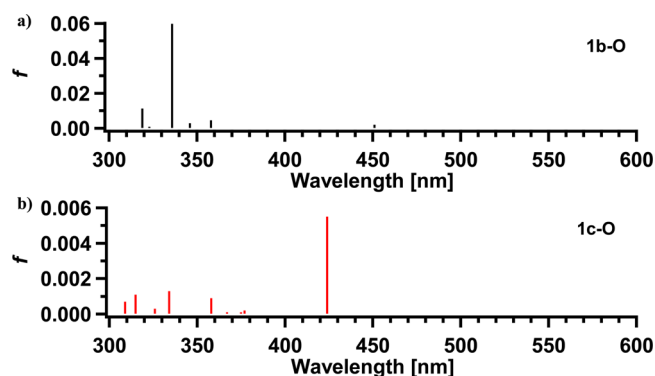


**Figure 12.** Calculated TD-DFT spectra for (a) **1b-O** and (b) **1c-O**.

methanol, and the decay rate constant of **1c-O** is only  $1.9 \times 10^5 \text{ s}^{-1}$  ( $\tau = 5.2 \mu\text{s}$ , Figure 13b), which is a reflection of **1c-O** decaying by abstracting H atom from the solvent to form **3** and **4**.

### 3. DISCUSSION

The triplet sensitized photolysis of **1** led to the formation of 1,2-biradical **1b**, which expels  $\text{N}_2$  to form triplet vinylnitrene **1c**. The transition state barrier for the extrusion of the  $\text{N}_2$  molecule is small enough that it takes place spontaneously at ambient temperature with a rate constant of  $3\text{--}5 \times 10^5 \text{ s}^{-1}$ . We have demonstrated that carbon-based radicals adjacent to the azido group lead to the expulsion of  $\text{N}_2$  to form imine radicals, and the rate constant for **6a** extruding  $\text{N}_2$  is faster than the time resolution of the laser flash photolysis apparatus, or  $6 \times 10^7 \text{ s}^{-1}$ .<sup>26</sup> The extrusion of  $\text{N}_2$  from **1b** is significantly slower than for **6a** (Scheme 8). Although, the calculated transition state barrier for **1b-O** extruding  $\text{N}_2$  molecule to form **1c-O** is higher than for **1b** expelling a  $\text{N}_2$  molecule to form **1c**, the rate for forming **1c-O** is faster than for **1c**, which supports the notion that addition of  $\text{O}_2$  and extrusion of  $\text{N}_2$  from **1b** take place concurrently, rather than stepwise.

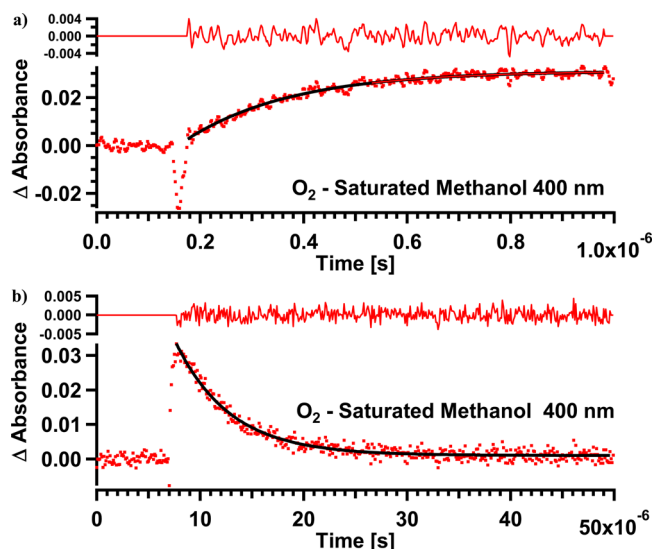
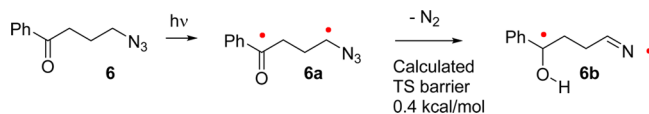


**Figure 13.** Kinetic trace recorded from laser flash photolysis of **1** in oxygen-saturated methanol at 400 nm over (a) 1  $\mu$ s and (b) 50  $\mu$ s time window.

#### Scheme 8



Interestingly, vinyl nitrene **1c** is significantly longer lived than previously reported vinyl nitrenes **7** and **8** that have lifetimes of a few  $\mu$ s at ambient temperature (Scheme 9). Because vinyl-

#### Scheme 9

	<b>1c</b>	<b>7</b>	<b>8</b>
Calculated Singlet Triplet Energy Gap (kcal/mol)	15	16	17
Lifetime in acetonitrile	1 ms	1.8 $\mu$ s	7 $\mu$ s
Calculated rotational barrier (kcal/mol)	14 and 16 (see Figure 3)	7.5	10

nitrenes **1c**, **7**, and **8** all decay by intersystem crossing to form the corresponding azirines, **1c** must intersystem cross slower than **7** and **8**. Wenthold showed that the singlet–triplet energy gap in vinyl nitrene can be reduced with electron delocalization;<sup>27</sup> however, the calculated energy gap between the triplet and singlet configuration of vinyl nitrenes **1c**, **7**, and **8** (Scheme 9) are similar and thus cannot be used to explain the difference in their lifetimes. We theorize, however, that intersystem crossing to the singlet surface of **1c** is facilitated by rotation around the C=C bond in vinyl nitrenes, which makes accessible higher-energy conformers with better spin-orbit coupling than the minimal energy conformer **1c**. In these high-energy conformers, the spins on the vinyl C and N atoms are in closer proximity and thus spin-orbit coupling is enhanced along with intersystem crossing. Further support for this notion comes from the calculated

rotational barriers for vinyl nitrenes **7** and **8**, which are smaller than that for **1c** and they are therefore shorter lived than **1c**. Thus, the intersystem crossing in vinyl nitrenes is similar to what has been proposed for intersystem crossing in 1,2-biradicals.<sup>28</sup>

As mentioned earlier, triplet vinyl nitrenes are unique as they react more efficiently with O<sub>2</sub> than triplet alkyl- and aryl nitrenes due to their 1,3-biradical character that places significant unpaired electron density on their  $\beta$ -carbon atom. Biradical **1b** also reacts efficiently with O<sub>2</sub> in acetonitrile and methanol, but with a rate constant that is significantly lower than for a diffusion-controlled process, or between 4 and  $5 \times 10^8$  M<sup>-1</sup> s<sup>-1</sup>, which is somewhat less than the reported rate constant for vinyl nitrenes **7** and **8** reacting with O<sub>2</sub>. Thus, biradical **1b** and vinyl nitrenes **7** and **8** are intercepted with O<sub>2</sub> with rate constants that are less than expected for a diffusional process, because they are electron-deficient biradicals due to their azido and nitreno substitution.

Photolysis of **1** in matrices led to  $\alpha$ -cleavage but not intersystem crossing to ketene imine or azirines as has been observed for most vinyl nitrenes in cryogenic matrices.<sup>6,29–34</sup> Thus, it seems reasonable to propose that vinyl nitrene **1c** is formed from vibrationally hot biradical **1b**, and it cleaves to form **1g** and **1h**. However, we cannot rule out the possibility that at cryogenic temperatures the  $\alpha$ -cleavage takes place from T<sub>1K</sub> of **1** that has ( $n,\pi^*$ ) configuration and the thermal population of T<sub>2K</sub> of **1** ( $\pi,\pi^*$ ) cannot compete with  $\alpha$ -cleavage from T<sub>1K</sub> of **1** ( $n,\pi^*$ ) as in solutions. Nevertheless, vinyl azide **1** displays unique reactivity in matrices.

## 4. CONCLUSIONS

We have shown that irradiation of vinyl azide **1**, which has a built-in triplet sensitizer, yields 1,2-biradical **1b** through intramolecular sensitization. Biradical **1b** reacts by expelling a N<sub>2</sub> molecule to form vinyl nitrene **1c**. Thus, triplet sensitization can be used to efficiently form triplet vinyl nitrene **1c** from vinyl azides **1**. Therefore, we conclude that triplet sensitization can be used to overcome the limitation of using vinyl azides as precursor for vinyl nitrenes, as intersystem crossing from the singlet excited states of vinyl azides and singlet vinyl nitrenes to their triplet configuration is inefficient. Intramolecular sensitization of vinyl azides can therefore be used in the pursuit of forming stable triplet vinyl nitrenes.

## 5. EXPERIMENTAL SECTION

**5.1. Calculations.** All geometries were optimized at the B3LYP level of theory and with 6-31G+(d) basis set as implemented in the Gaussian03 programs.<sup>17–19</sup> All transition states were confirmed to have one imaginary vibrational frequency. Intrinsic reaction coordinate calculations were used to verify that the located transition states corresponded to the attributed reactant and product.<sup>35,36</sup> The absorption spectra were calculated using time-dependent density functional theory (TD-DFT).<sup>37–41</sup>

**5.2. Synthesis.** *Synthesis of 3-Methyl-1-phenyl-but-3-en-1-ol.* The method of Imai and Nishida was followed to make this compound.<sup>42</sup> To a magnetically stirred solution of benzaldehyde (5.3 g, 50 mmol) and 3-chloro-2-methylpropene (5.4 g, 60 mmol) in dimethylformamide (DMF) (100 mL) was added successively SnCl<sub>4</sub>·2H<sub>2</sub>O (17 g, 75 mmol) and NaI (11 g, 75 mmol); a mild exothermic reaction was noted at the early stage. After stirring for 20 h at room temperature, 30% aqueous NH<sub>4</sub>F (100 mL) and diethyl ether (200 mL) were added. The mixture was stirred, and the two layers separated. The aqueous phase was re-extracted with diethyl ether. The ether extracts were combined, washed with saturated aqueous NaCl (100 mL), and dried over MgSO<sub>4</sub>. The removal of solvent yielded 3-methyl-1-phenyl-but-3-en-1-ol (7.6 g, 47 mmol, 95% yield). IR (neat): 3410, 1640, 910 cm<sup>-1</sup>; <sup>1</sup>H NMR (CDCl<sub>3</sub>, 250 MHz): 1.77 (s, 3H), 2.31 (s, 1H), 2.40 (d,



2H, 6.8 Hz), 4.76 (t, 1H, 6.8 Hz), 4.82 (s, 1H), 4.89 (s, 1H), 7.21–7.40 (m, 5H) ppm. MS (*m/e*): 162 (*M*<sup>+</sup>, <1%).

**Synthesis of 3-Methyl-1-phenyl-but-3-en-1-one.**<sup>43</sup> To a stirred slurry of 3-methyl-1-phenyl-but-3-en-1-ol (7.6 g, 47 mmol) in acetone (100 mL) was added Jones reagent (10 g of chromium trioxide, 10 mL of sulfuric acid, and 30 mL of water) until the color changed to an orangish-yellow solution. The solution was filtered and the acetone was removed in vacuo to give a red-brown slurry that was dissolved in diethyl ether (250 mL), and then the ether layer was washed with saturated sodium bicarbonate solution and dried (MgSO<sub>4</sub>). Removal of the diethyl ether in vacuo at room temperature produced 3-methyl-1-phenyl-but-3-en-1-one (6.08 g, 38 mmol, 80% yield). IR (neat): 3076, 2971, 2913, 1687, 1448, 1207, 690 cm<sup>-1</sup>. <sup>1</sup>H NMR (CDCl<sub>3</sub>, 250 MHz): 7.99 (d, 2H, 8 Hz), 7.56 (t, 1H, 7 Hz), 7.48 (d, 2H, 8 Hz) 4.98 (s, 1H), 4.85 (s, 1H), 3.68 (s, 2H), 1.82 (s, 3H) ppm. MS (*m/e*): 160 (*M*<sup>+</sup>, <1%).

**Synthesis of 4-Azido-3-iodo-3-methyl-1-phenylbutanone.** The azido-iodo compound was prepared following the procedure of Molina et al.<sup>44</sup> To a stirred slurry of sodium azide (6.0 g, 0.087 mol) in acetonitrile (100 mL) at -10 °C was added slowly iodine monochloride (6.56 g, 0.04 mol) over a period of 20 min. The reaction mixture was stirred for an additional 5–10 min, and 3-methyl-1-phenyl-but-3-en-1-one (6.08 mg, 0.038 mol) was added, allowed to warm to room temperature, and stirred for 8–20 h. The red-brown slurry was poured into water (250 mL), and the mixture was extracted with diethyl ether (250 mL) in three portions. These were combined and washed with 5% sodium thiosulfate (150 mL), leaving a colorless ethereal solution. The solution was washed with water (900 mL) in four portions and dried over magnesium sulfate. Removal of the diethyl ether in vacuo at room temperature produced the iodo-azide adduct (7.42 g, 0.022 mol, 60% yield), slightly orange in color. IR (neat): 2104, 1688, 1596, 1580, 1448, 1221, 1002 cm<sup>-1</sup>.

4-Azido-3-methyl-1-phenyl-but-3-en-1-one (7.4 g, 0.02 mol) was reacted with sodium azide (1.5 g, 0.022 mol) in dimethylformamide (100 mL, dried over molecular sieves, type 4 Å) at room temperature. The solution was then poured into a mixture of water-diethyl ether, and the diethyl ether layer was washed several times with water and dried over MgSO<sub>4</sub>. Removal of the diethyl ether yielded a mixture of *cis*- and *trans*-azido-3-methyl-1-phenyl-but-3-en-1-one (2.7 g, 13.3 mmol, 60% yield). The crude product was purified by column chromatography using an ethyl acetate and hexane system in the increasing order of polarity to yield *E*-form (540 mg, 2.6 mmol, 20% yield) and *Z*-form (324 mg, 1.6 mmol, 12% yield) of 4-azido-3-methyl phenyl-but-3-en-1-one.

***E*-4-Azido-3-methyl-1-phenyl-but-3-en-1-one.** IR (neat): 2105, 1675, 1600, 1574, 1510, 1259, 1170 cm<sup>-1</sup>. <sup>1</sup>H NMR (CDCl<sub>3</sub>, 250 MHz): 7.96 (d, 2H, 8 Hz), 7.57 (t, 1H, 7 Hz), 7.46 (t, 2H, 8 Hz), 6.10 (s, 1H), 3.62 (s, 2H), 1.69 (s, 3H) ppm. <sup>13</sup>C NMR (CDCl<sub>3</sub>, 250 MHz): 18, 40, 121, 123.16, 128, 128, 133, 136, 196 ppm. HRMS: Calculated for C<sub>11</sub>H<sub>12</sub>N<sub>3</sub>O = 202.0980. Found = 202.0980. HRMS = high-resolution mass spectrometry.

***Z*-4-Azido-3-methyl-1-phenyl-but-3-en-1-one.** IR (neat): 2100, 1682, 1605, 1479, 1449, 1010 cm<sup>-1</sup>. <sup>1</sup>H NMR (CDCl<sub>3</sub>, 250 MHz): 8.0 (d, 2H, 8 Hz), 7.57 (t, 1H, 7 Hz), 7.46 (t, 2H, 8 Hz), 6.17 (s, 1H), 3.72 (s, 2H), 1.71 (s, 3H) ppm. <sup>13</sup>C NMR (CDCl<sub>3</sub>, 250 MHz): 15, 45, 123, 124, 128, 128, 133, 136, 197 ppm.

**5.3. Photolysis of *E*-4-Azido-3-methylphenyl-but-3-en-1-one.** **Photolysis in Argon-Saturated Solution.** A solution of *E*-4-azido-3-methylphenyl-but-3-en-1-one (20 mg, 0.0995 mmol) in toluene (3 mL, dried over Na) was bubbled with argon for 20 min and photolyzed for 50 min ( $\lambda > 312$  nm). The reaction was monitored with thin-layer chromatography (TLC). Evaporation of toluene yielded 2-(2-methyl-2H-azirin-2-yl)-1-phenyl ethanone (16.4 mg, 95 mmol, 82% yield) and the starting material **1** (1.8 mg, 9 mmol, 8% yield). The photoproduct was characterized by NMR, HRMS, and IR spectroscopy. IR (neat): 3060, 2975, 2952, 2922, 2107, 1683, 1640, 1597, 1579, 1448 cm<sup>-1</sup>. <sup>1</sup>H NMR (CDCl<sub>3</sub>, 400 MHz): 10.2 (s, 1H), 7.88 (d, 2H, 7 Hz), 7.54 (t, 1H, 7 Hz), 7.46 (d, 2H, 7 Hz), 3.42 (d, 1H, 16 Hz), 3.07 (d, 1H, 16 Hz), 1.35 (s, 3H) ppm. <sup>13</sup>C NMR (CDCl<sub>3</sub>, 400 MHz): 197, 173, 136, 133, 128, 124, 47, 28, 24 ppm. HRMS (*M*+H); Calculated for C<sub>11</sub>H<sub>12</sub>N<sub>1</sub>O = 174.0919. Found = 174.0914.

**Photolysis in Oxygen-Saturated Solutions.** A solution of *E*-4-azido-3-methylphenyl-but-3-en-1-one (20 mg, 0.0995 mmol) in toluene (3 mL, dried over Na) was bubbled with oxygen for 30 min and photolyzed for 30 min through a Pyrex filter. The reaction was monitored with high-performance liquid chromatography (HPLC), and irradiation was stopped when 15% of the precursor had reacted. Analysis of the HPLC trace showed formation of two products in the ratio of 2:1.

A solution of *E*-4-azido-3-methylphenyl-but-3-en-1-one (124 mg, 0.614 mmol) in dry distilled toluene (24 mL) was photolyzed for 30 min (Pyrex filter). Removal of solvent in vacuum, followed by isolation using HPLC, yielded 2-hydroxy-2-methyl-4-oxo-4-phenylbutyronitrile **3** (4 mg, 0.021 mmol, 3% yield) and (*E*)-2-methyl-4-oxo-4-phenyl-but-2-enitrile **4** (2 mg, 0.011 mmol, 1.6% yield) and recovered the starting material. The spectroscopic characterizations of **3** and **4** fit with those in the literature.<sup>45,46</sup>

**Compound 3.**<sup>45</sup> IR (CDCl<sub>3</sub>): 3455, 3063, 2992, 2919, 1681, 1597, 1580 cm<sup>-1</sup>. <sup>1</sup>H NMR (CDCl<sub>3</sub>): 1.752 (s, 3H), 3.25 (d, 1H, 18 Hz), 3.723 (d, 1H, 18 Hz), 5.169 (s, 1H), 0.5.61 (t, 2H, 8 Hz), 7.69 (t, 1H, 7 Hz), 7.99 (d, 2H, 8 Hz) ppm. <sup>13</sup>C NMR (CDCl<sub>3</sub>): 198, 135, 134, 129, 128, 121, 65, 47, 27 ppm. HRMS: Calculated mass (*M*+23) = 212.0687. Experimental (*M*+23) = 212.0684.

**Compound 4.**<sup>46</sup> IR (CDCl<sub>3</sub>): 3061, 2920, 2850, 2219, 1669, 1609, 1596, 1579 cm<sup>-1</sup>. <sup>1</sup>H NMR (CDCl<sub>3</sub>): 2.304 (s, 3H), 7.421 (s, 1H), 7.55 (t, 1H, 8 Hz), 7.67 (t, 1H, 7 Hz), 8.0 (d, 2H, 8 Hz) ppm.

**5.4. Laser Flash Photolysis.** Laser flash photolysis experiments were done with a YAG laser (355 and 266 nm, 15 ns)<sup>47</sup> or an excimer laser (308 nm, 17 ns).<sup>26</sup> Stock solutions of **1** in methanol or acetonitrile were prepared with spectroscopic-grade solvents such that the solutions had an absorption between 0.2 and 0.8 at the excitation wavelengths. Solutions were purged with nitrogen or oxygen for at least 15 min. Solutions of **1** are relatively photolabile and could be excited only with a small number of laser shots. For this reason, transient spectra were collected using a flow system, where a freshly prepared solution was pumped through a custom-designed Suprasil-cell (7 × 7 mm) at a rate of 1.5–2.0 mL/min. As a result, a fresh solution was irradiated by each laser shot. Decays were collected either by using the flow system or by subjecting the sample in static cells to a small number of laser shots and checking for the integrity of the sample with UV-vis spectroscopy. The kinetic traces were fitted so the chi square value (the ratio of the curve fitting error to the standard deviation) is typically <0.02% of standard deviation of the measured data.

**5.5. Matrix Isolation.** Matrix isolation studies were performed using conventional equipment.<sup>48</sup>

**5.6. X-ray Crystallography.** Single crystals were obtained as colorless plates from Et<sub>2</sub>O. For X-ray examination and data collection, a suitable crystal, approximate dimensions 0.12 × 0.11 × 0.01 mm, was mounted in a loop with paratone-N and transferred immediately to the goniostat bathed in a cold stream. Intensity data were collected at 200 K on a D8 goniostat equipped with a Bruker Platinum 200 CCD detector at Beamline 11.3.1 at the Advanced Light Source (Lawrence Berkeley National Laboratory) using synchrotron radiation tuned to  $\lambda = 0.77490$  Å. For data collection, frames were measured for a duration of 2 s at 0.3° intervals of  $\omega$ . The data frames were collected using the APEX2 suite of programs. The data were corrected for absorption and beam corrections based on the multiscan technique as implemented in SADABS. The structure was solved by a combination of direct methods in SHELXTL and the difference Fourier technique and refined by full-matrix least-squares on F<sup>2</sup>. Non-hydrogen atoms were refined with anisotropic displacement parameters. The H atoms were calculated and treated with a riding model. The H atom isotropic displacement parameters were defined as  $a^*U_{eq}(C)$  of the adjacent atom ( $a = 1.5$  for CH<sub>3</sub> and 1.2 for all others). The refinement converged with crystallographic agreement factors of R1 = 4.51%, wR2 = 11.49% for 2368 reflections with  $I > 2\sigma(I)$  (R1 = 6.00%, wR2 = 12.45% for all data) and 274 variable parameters.

## ■ ASSOCIATED CONTENT

### ■ Supporting Information

NMR and IR spectra of 1–3. Cartesian coordinates, energies, and vibrational frequencies are included. This material is available free of charge via the Internet at <http://pubs.acs.org>.

## ■ AUTHOR INFORMATION

### Corresponding Author

\*E-mail: [anna.gudmundsdottir@gmail.com](mailto:anna.gudmundsdottir@gmail.com).

### Notes

The authors declare no competing financial interest.

## ■ ACKNOWLEDGMENTS

We thank the National Science Foundation and the Ohio Supercomputer Center for supporting this work. S.R. thanks the U. C. Chemistry Department for a Twitchell fellowship, and Q. L. thanks the Zimmer program for their support. C. B., R. L., and T. C. S. P. thank the Natural Sciences and Engineering Council of Canada (NSERC) for support in the form of a discovery grant (C. B.) and a CGS-D fellowship (T. C. S. P.). Crystallographic data were collected through the SCrALS (Service Crystallography at Advanced Light Source) program at Beamline 11.3.1 at the Advanced Light Source (ALS), Lawrence Berkeley National Laboratory. The ALS is supported by the Director, Office of Science, Office of Basic Energy Sciences, of the U.S. Department of Energy under Contract No. DE-AC02-05CH11231.

## ■ REFERENCES

- (1) *Nitrenes and Nitrenium Ions*; Falvey, D. E.; Gudmundsdottir, A. D., Eds. Wiley Ser. React. Intermed. Chem. Biol., Vol. 6; John Wiley & Sons, Inc.: New York, 2013.
- (2) Platz, M. S. In *Reactive Intermediate Chemistry*; Moss, R. A., Platz, M. S., Jones, M., Jr., Eds.; John Wiley & Sons, Inc.: New York, 2004.
- (3) Rajam, S.; Murthy, R. S.; Jadhav, A. V.; Li, Q.; Keller, C.; Carra, C.; Pace, T. C. S.; Bohne, C.; Ault, B. S.; Gudmundsdottir, A. D. *J. Org. Chem.* **2011**, *76*, 9934.
- (4) Gamage, D. W.; Li, Q.; Ranaweera, R. A. A. U.; Sarkar, S. K.; Weragoda, G. K.; Carr, P. L.; Gudmundsdottir, A. D. *J. Org. Chem.* **2013**, *78*, 11349.
- (5) Zhang, X.; Sarkar, S. K.; Weragoda, G. K.; Rajam, S.; Ault, B. S.; Gudmundsdottir, A. D. *J. Org. Chem.* **2014**, *79*, 653.
- (6) Nunes, C. M.; Reva, I.; Pinho e Melo, T. M. V. D.; Fausto, R.; Šolomek, T.; Bally, T. *J. Am. Chem. Soc.* **2011**, *133*, 18911.
- (7) Parasuk, V.; Cramer, C. J. *Chem. Phys. Lett.* **1996**, *260*, 7.
- (8) Singh, P. N. D.; Mandel, S. M.; Sankaranarayanan, J.; Muthukrishnan, S.; Chang, M.; Robinson, R. M.; Lahti, P. M.; Ault, B. S.; Gudmundsdottir, A. D. *J. Am. Chem. Soc.* **2007**, *129*, 16263.
- (9) Li, Y. Z.; Kirby, J. P.; George, M. W.; Poliakoff, M.; Schuster, G. B. *J. Am. Chem. Soc.* **1988**, *110*, 8092.
- (10) Sankaranarayanan, J.; Bort, L. N.; Mandel, S. M.; Chen, P.; Krause, J. A.; Brooks, E. E.; Tsang, P.; Gudmundsdottir, A. D. *Org. Lett.* **2008**, *10*, 937.
- (11) Leyva, E.; Platz, M. S.; Persy, G.; Wirz, J. *J. Am. Chem. Soc.* **1986**, *108*, 3783.
- (12) Buron, C.; Platz, M. S. *Org. Lett.* **2003**, *5*, 3383.
- (13) Wijeratne, N. R.; Da Fonte, M.; Ronemus, A.; Wyss, P. J.; Tahmassebi, D.; Wenthold, P. G. *J. Phys. Chem. A* **2009**, *113*, 9467.
- (14) Gritsan, N. P.; Tigelaar, D.; Platz, M. S. *J. Phys. Chem. A* **1999**, *103*, 4465.
- (15) Singh, P. N. D.; Mandel, S. M.; Robinson, R. M.; Zhu, Z.; Franz, R.; Ault, B. S.; Gudmundsdottir, A. D. *J. Org. Chem.* **2003**, *68*, 7951.
- (16) Travers, M. J.; Cowles, D. C.; Clifford, E. P.; Ellison, G. B.; Engelking, P. C. *J. Chem. Phys.* **1999**, *111*, 5349.
- (17) Gaussian 03. Frisch, M. J.; Trucks, G. W.; Schlegel, H. B.; Scuseria, G. E.; Robb, M. A.; Cheeseman, J. R.; Montgomery, J. A., Jr.

- Vreven, T.; Kudin, K. N.; Burant, J. C.; Millam, J. M.; Iyengar, S. S.; Tomasi, J.; Barone, V.; Mennucci, B.; Cossi, M.; Scalmani, G.; Rega, N.; Petersson, G. A.; Nakatsuji, H.; Hada, M.; Ehara, M.; Toyota, K.; Fukuda, R.; Hasegawa, J.; Ishida, M.; Nakajima, T.; Honda, Y.; Kitao, O.; Nakai, H.; Klene, M.; Li, X.; Knox, J. E.; Hratchian, H. P.; Cross, J. B.; Adamo, C.; Jaramillo, J.; Gomperts, R.; Stratmann, R. E.; Yazyev, O.; Austin, A. J.; Cammi, R.; Pomelli, C.; Ochterski, J. W.; Ayala, P. Y.; Morokuma, K.; Voth, G. A.; Salvador, P.; Dannenberg, J. J.; Zakrzewski, V. G.; Dapprich, S.; Daniels, A. D.; Strain, M. C.; Farkas, O.; Malick, D. K.; Rabuck, A. D.; Raghavachari, K.; Foresman, J. B.; Ortiz, J. V.; Cui, Q.; Baboul, A. G.; Clifford, S.; Cioslowski, J.; Stefanov, B. B.; Liu, G.; Liashenko, A.; Piskorz, P.; Komaromi, I.; Martin, R. L.; Fox, D. J.; Keith, T.; Al-Laham, M. A.; Peng, C. Y.; Nanayakkara, A.; Challacombe, M. G.; Gill, P. M. W.; Johnson, B.; Chen, W.; Wong, M. W.; Gonzalez, C.; Pople, J. A. Gaussian, Inc.: Wallingford, CT, 2003.
- (18) Becke, A. D. *Chem. Phys.* **1993**, *98*, 5648.
- (19) Lee, C.; Yang, W.; Parr, R. G. *Phys. Rev. B* **1988**, *37*, 785.
- (20) Murov, S. L.; Carmichael, I.; Hug, G. L. *Handbook of Photochemistry*; Marcel Dekker: New York, 1993.
- (21) Muthukrishnan, S.; Mandel, S. M.; Hackett, J. C.; Singh, P. N. D.; Hadad, C. M.; Krause, J. A.; Gudmundsdottir, A. D. *J. Org. Chem.* **2007**, *72*, 2757.
- (22) Srivastava, S.; Yourd, E.; Toscano, J. P. *J. Am. Chem. Soc.* **1998**, *120*, 6173.
- (23) Neville, A. G.; Brown, C. E.; Rayner, D. M.; Lusztyk, J.; Ingold, K. U. *J. Am. Chem. Soc.* **1991**, *113*, 1869.
- (24) Wentrup, C. *Aust. J. Chem.* **2013**, *66*, 852.
- (25) Gritsan, N. P.; Platz, M. S. In *Organic Azides: Syntheses and Applications*; Brase, S., Banert, K., Eds.; John Wiley & Sons, Ltd: Chippingham, Wiltshire, U.K., 2010.
- (26) Muthukrishnan, S.; Sankaranarayanan, J.; Klima, R. F.; Pace, T. C. S.; Bohne, C.; Gudmundsdottir, A. D. *Org. Lett.* **2009**, *11*, 2345.
- (27) Wenthold, P. G. *J. Org. Chem.* **2012**, *77*, 208.
- (28) Caldwell, R. A.; Carlacci, L.; Doubleday, C. E., Jr.; Furlani, T. R.; King, H. F.; McIver, J. W., Jr. *J. Am. Chem. Soc.* **1988**, *110*, 6901.
- (29) Inui, H.; Murata, S. *Chem. Commun.* **2001**, 1036.
- (30) Murata, S.; Tomioka, H. *Chem. Lett.* **1992**, 57.
- (31) Nunes, C. M.; Reva, I.; Fausto, R. *J. Org. Chem.* **2013**, *78*, 10657.
- (32) Bégué, D.; Dargelos, A.; Berstermann, H. M.; Netsch, K. P.; Bednarek, P.; Wentrup, C. *J. Org. Chem.* **2014**, *79*, 1247.
- (33) Kvaskoff, D.; Vosswinkel, M.; Wentrup, C. *J. Am. Chem. Soc.* **2011**, *133*, 5413.
- (34) Wentrup, C. *Wiley Ser. React. Intermed. Chem. Biol.* **2013**, *6*, 273.
- (35) Gonzalez, C.; Schlegel, H. B. *J. Chem. Phys.* **1989**, *90*, 2154.
- (36) Gonzalez, C.; Schlegel, H. B. *J. Phys. Chem.* **1990**, *94*, 5523.
- (37) *Density Functional Methods in Chemistry*; Labanowski, J. K., Andzelm, J. W., Eds.; Springer-Verlag: New York, 1991.
- (38) Parr, R. G.; Weitao, Y. *Density Functional Theory in Atoms and Molecules*; Oxford University Press: Oxford, U.K., 1989.
- (39) Bauernschmitt, R.; Ahlrichs, R. *Chem. Phys. Lett.* **1996**, *256*, 454.
- (40) Stratmann, R. E.; Scuseria, G. E.; Frisch, M. J. *J. Chem. Phys.* **1998**, *109*, 8218.
- (41) Foresman, J. B.; Head-Gordon, M.; Pople, J. A.; Frisch, M. J. *J. Phys. Chem.* **1992**, *96*, 135.
- (42) Imai, T.; Nishida, S. *Synthesis* **1993**, 1993, 395.
- (43) Rieke, R. D.; Klein, W. R.; Wu, T. C. *J. Org. Chem.* **1993**, *58*, 2492.
- (44) Molina, P.; Pastor, A.; Vilaplana, M. J.; Foces-Foces, C. *Tetrahedron* **1995**, *51*, 1265.
- (45) Soldermann, C. P.; Vallinayagam, R.; Tzouros, M.; Neier, R. *J. Org. Chem.* **2008**, *73*, 764.
- (46) Trabulsi, H.; Rousseau, G. *Synth. Commun.* **2011**, *41*, 2123.
- (47) Liao, Y.; Bohne, C. *J. Phys. Chem.* **1996**, *100*, 734.
- (48) Ault, B. S. *J. Am. Chem. Soc.* **1978**, *100*, 2426.